

Dispersive Metasurface Sheet Analysis Using GSTC-FDTD

Yousef Vahabzadeh, Nima Chamanara and Christophe Caloz, *Fellow, IEEE*

Abstract—Metasurfaces are zero thickness structures and represent general electromagnetic discontinuity. Conventional boundary conditions, and therefore computational techniques, cannot handle such discontinuities. Generalized Sheet Transition Conditions (GSTCs) have been developed for their modeling. In this paper, we propose a scheme based on FDTD for efficient simulation of dispersive metasurfaces which is extension of our previous works on space-time varying metasurfaces. The scheme is proved by two illustrative examples.

Index Terms—Metasurface, Generalized Sheet Transition Condition (GSTC), General Discontinuity, FDTD, dispersive metasurface.

I. INTRODUCTION

Metasurfaces [1]–[3] are 2D planar structures, very thin compared to the operation wavelength, made of all-dielectric unit cells or periodic arrays of metallic inclusions on a thin substrate. Compared to the conventional 3D metamaterial, they are less lossy and easy to fabricate [4]. They have many applications such as, for example, high resolution imaging [5], vectorial beam generation [6], [7], field focusing [8]. Moreover, they are capable of performing several transformations for the given incident wave(s) into the desired reflected and transmitted waves [9].

In fact, since their thickness are very small compared to the wavelength, $\delta \ll \lambda_0$, they are modeled as a zero-thickness sheet [10]. Therefore, it makes both of the electric and magnetic fields discontinuous in space, general discontinuity [1], [11]. Moreover, they are bi-anisotropic structures in general, thus, they are the most general form of the electromagnetic discontinuity. Generalized Sheet Transition Conditions [12], GSTCs, are developed for modeling such discontinuities [13].

Conventional numerical electromagnetic techniques and, therefore, commercial softwares are not capable of simulating sheet discontinuities. For this reason, many

Y. Vahabzadeh, N. Chamanara and C. Caloz are with the Department of Electrical Engineering, École Polytechnique de Montréal, Montréal, QC, H3T 1J4 Canada (e-mail:).

Manuscript received MONTH XX, 2016; revised MONTH XX, 2016.

works have been done in the literature to efficiently model those discontinuities. In [14] and [15] a technique was developed based on finite difference and Finite element schemes, respectively, for their modeling in frequency domain. A limitation of these techniques is being monochromatic. Therefore, in [16] a technique based on FDTD scheme was developed which enables polychromatic simulation for isotropic Lorentzian metasurface. Using this technique any other dispersion forms should be extended by many Lorentzians. However, since Lorentzians doesn't make a complete set, therefore, it is limited regarding the dispersion simulation capability and in some cases many Lorentzian are required in the series. In [17] we developed a fully numeric technique based on FDTD where the conventional FDTD equations are modified to efficiently simulate space-time varying metasurfaces. However, this technique is not applicable for any kind of dispersive metasurfaces. In this paper, we are extending the method of [17] for the simulation of general bi-anisotropic dispersive metasurface.

The structure of the paper is as follows: In section II, metasurface frequency domain synthesis equation is recalled. In the next section, different types of dispersive metasurfaces are discussed. Section IV, is the core part of the paper where the integration of GSTC in the FDTD technique for analyzing metasurface sheets is detailed. In the last section, section V, two illustrative examples are shown to verify the formulation of the previous section. Finally, conclusion is made.

II. RECALL OF METASURFACE GSTC SYNTHESIS EQUATIONS

The metasurface, Fig. 1, synthesis equations, assuming zero normal polarization densities, developed in [9], [12], [13] are as follows

$$\begin{pmatrix} -\Delta \tilde{H}_z \\ \Delta \tilde{H}_y \end{pmatrix} = j\omega \varepsilon_0 \begin{pmatrix} \tilde{\chi}_{ee}^{yy} & \tilde{\chi}_{ee}^{yz} \\ \tilde{\chi}_{ee}^{zy} & \tilde{\chi}_{ee}^{zz} \end{pmatrix} \begin{pmatrix} \tilde{E}_{y,av} \\ \tilde{E}_{z,av} \end{pmatrix} \quad (1a)$$

$$+ j\omega \sqrt{\varepsilon_0 \mu_0} \begin{pmatrix} \tilde{\chi}_{em}^{yy} & \tilde{\chi}_{em}^{yz} \\ \tilde{\chi}_{em}^{zy} & \tilde{\chi}_{em}^{zz} \end{pmatrix} \begin{pmatrix} \tilde{H}_{y,av} \\ \tilde{H}_{z,av} \end{pmatrix},$$

$$\begin{pmatrix} -\Delta\tilde{E}_y \\ \Delta\tilde{E}_z \end{pmatrix} = j\omega\mu_0 \begin{pmatrix} \tilde{\chi}_{\text{mm}}^{zz} & \tilde{\chi}_{\text{mm}}^{zy} \\ \tilde{\chi}_{\text{mm}}^{yz} & \tilde{\chi}_{\text{mm}}^{yy} \end{pmatrix} \begin{pmatrix} \tilde{H}_{z,\text{av}} \\ \tilde{H}_{y,\text{av}} \end{pmatrix} \quad (1b)$$

$$+ j\omega\sqrt{\varepsilon_0\mu_0} \begin{pmatrix} \tilde{\chi}_{\text{me}}^{zz} & \tilde{\chi}_{\text{me}}^{zy} \\ \tilde{\chi}_{\text{me}}^{yz} & \tilde{\chi}_{\text{me}}^{yy} \end{pmatrix} \begin{pmatrix} \tilde{E}_{z,\text{av}} \\ \tilde{E}_{y,\text{av}} \end{pmatrix},$$

where $\Delta\tilde{\psi} = \tilde{\psi}^{\text{tr}} - (\tilde{\psi}^{\text{inc}} + \tilde{\psi}^{\text{ref}})$ and $\Delta\tilde{\psi} = \frac{\tilde{\psi}^{\text{tr}} + (\tilde{\psi}^{\text{inc}} + \tilde{\psi}^{\text{ref}})}{2}$ with $\tilde{\psi}$ representing any component of the frequency domain \tilde{E} or \tilde{H} fields and tr, inc and ref standing for transmitted, incident and reflected fields, respectively. Using this equation, for the specified incident, reflected and transmitted fields, the corresponding susceptibilities can be calculated. Since number of unknowns, susceptibilities, is more than number known – specified – fields, therefore, there is possibility of performing several transformations.

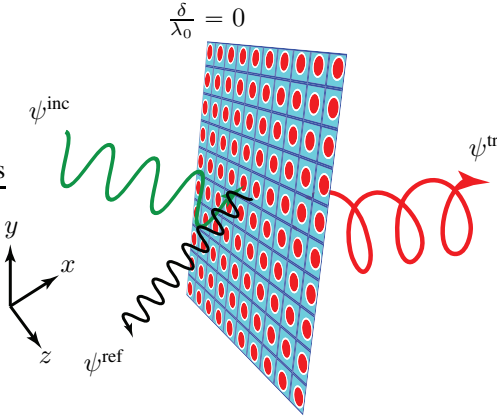


Fig. 1: Metasurface sheet discontinuity (zero thickness, $\frac{\delta}{\lambda_0} = 0$), transforming a given incident wave (ψ^{inc}) into a reflected (ψ^{ref}) and transmitted (ψ^{tr}) wave.

III. DISPERSIVE METASURFACE

Dispersive metasurfaces are structures that their susceptibilities can vary in frequency. A simple form of dispersion can be $\frac{h}{j\omega}$, where h is a constant and ω is the angular frequency. This form of the dispersion appears in the design of reflection-less metasurfaces with a given transmission coefficient, T . For example, $h = -2c_0$ and $h = -\frac{2}{3}$ results in absorbing and half-wave transmitting metasurface [17], respectively. Other most useful types of dispersive metasurfaces can be Lorentzian and Debye dispersion or combination of them.

Assuming $\exp(j\omega t)$, susceptibility representation of a single pole Debye dispersive medium is

$$\tilde{\chi}_D(\omega) = \frac{\Delta\tilde{\varepsilon}_p}{1 + j\omega\tau_p}, \quad (2)$$

where $\Delta\tilde{\varepsilon}_p = \varepsilon_0 - \varepsilon_\infty$ with ε_0 and ε_∞ showing the zero frequency and infinite frequency permittivities [18].

Susceptibility representation of a single pole pair Lorenzian dispersive metasurfaces is

$$\tilde{\chi}_L(\omega) = \frac{\Delta\tilde{\varepsilon}_p\omega_p^2}{\omega_p^2 + 2j\omega\delta_p - \omega^2}, \quad (3)$$

where ω_p is the frequency of the pole pair [18].

Using the technique presented in [17], $\frac{h}{j\omega}$ form of dispersion can be simulated. However, it has limitations regarding dispersion simulation such as Lorentzian and Debye dispersions, or combination of them. In the next section, we will focus on the simulation of these types of dispersive metasurfaces. The same technique is applicable to other casual dispersive functions.

IV. GSTC-FDTD FOR DISPERSIVE METASURFACE

To avoid tedious and long mathematical calculations and without loss of generality, we consider 1D problem of bi-anisotropic metasurface with $(E_z, H_y) \neq 0$ (TEM-mode) and $\mathbf{k} = k_0\hat{x}$. For the 2D and 3D problems, exactly the same technique that will be elaborated upon here is applicable and is not repeated here.

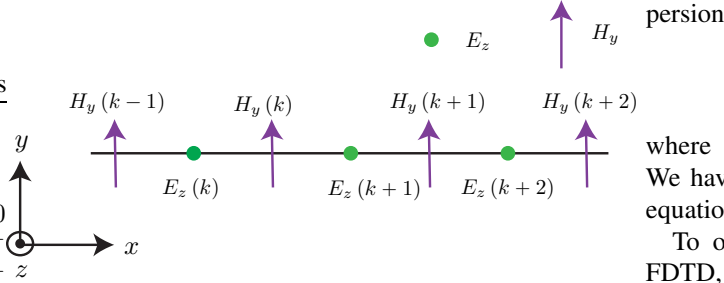
From [18] the FDTD equation for the mentioned TEM mode reads

$$H_y^{n+\frac{1}{2}}(i) = H_y^{n-\frac{1}{2}}(i) + \frac{\Delta t}{\mu_0\Delta x} [E_z^n(i+1) - E_z^n(i)], \quad (4a)$$

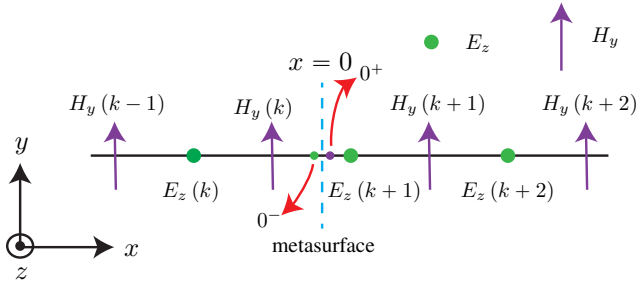
$$E_z^n(i) = E_z^{n-1}(i) + \frac{\Delta t}{\varepsilon_0\Delta x} [H_y^{n-\frac{1}{2}}(i) - H_y^{n-\frac{1}{2}}(i-1)] \quad (4b)$$

The space grid is shown in Fig. 2a. The next step is to position the metasurface in the solving region. As mentioned before, the metasurface is zero thickness and makes both E and H fields discontinuous. Positioning the metasurface on the E-field nodes can represent only H-field discontinuity and E-field will be continuous as discussed in [19] for the analysis of graphene sheet. Similarly, position on H-field grid nodes gives only discontinuity of the electric field. Therefore, as proposed in [17], the best solution is to position the metasurface between the two neighboring cells as shown in Fig. 2b.

Everywhere in the space (4) can be employed to update the fields and march on time. However, for the nodes around the metasurface, $E_z(k+1)$ and $H_y(k)$, a special treatment is required to include the effect of the discontinuity in the update equations. First consider update equation for $E_z(k+1)$ where $H_y(k)$ and $H_y(k+1)$ are involved with the former being at the other side of the discontinuity. Therefore, to include the effect of the discontinuity, as shown in Fig. 2b, a magnetic virtual



(a) Regular FDTD Yee grid nodes.



(b) Yee FDTD grid nodes with the virtual nodes.

Fig. 2: 1D FDTD Yee grid with and without the metasurface. In Fig. 2b, the metasurface is placed between the two cells, k and $k+1$. The filled small green and purple circles represent electric and magnetic virtual nodes just before ($x = 0^-$) and after ($x = 0^+$) the metasurface, respectively. The metasurface is illuminated from the left in x -direction.

node is considered at the same side of the $E_z(k+1)$. Addition of this node solves the problem of existing discontinuity between the nodes. Therefor the update equation for $E_z(k+1)$ will be

$$E_z^n(k+1) = E_z^{n-1}(k+1) + \frac{\Delta t}{\varepsilon_0 \Delta x} [H_y^{n-\frac{1}{2}}(k+1) - H_y^{n-\frac{1}{2}}(0^+)]. \quad (5)$$

Similarly, a virtual electric node is considered at $x = 0^-$ to update $H_y(k)$ and instead of $E_z(k+1)$, $E_z(0^-)$ is used. With this scheme (4a) will be

$$H_y^{n+\frac{1}{2}}(k) = H_y^{n-\frac{1}{2}}(k) + \frac{\Delta t}{\mu_0 \Delta x} [E_z^n(0^-) - E_z^n(k)]. \quad (6)$$

The next step is to calculate $H_y(0^+)$ and $E_z(0^-)$ for which the GSTC equations are used. However, because of the dispersive nature of the metasurface, (1) cannot be discretized in time domain. Therefore, we introduce auxiliary P and M functions to solve the issue.

We assume electric and magnetic susceptibilities of the dispersive metasurface are given by Lorentzian dis-

$$\tilde{\chi}_{L,kk}(\omega) = \frac{\Delta \varepsilon_p \omega_{p,kk}^2}{\omega_{p,kk}^2 + 2j\omega \delta_{p,kk} - \omega^2}, \quad (7)$$

where $k = e$ or m and $kk=ee$ or em or me or mm . We have dropped the superscripts for readability of the equations.

To obtain the time domain equation for use in the FDTD, we substitute (7) in (1). We consider general bi-anisotropic metasurface ($\chi_{ee}^{zz}, \chi_{em}^{yy}, \chi_{me}^{zz}, \chi_{mm}^{yy} \neq 0$). Other susceptibilities are not effective as $H_z = E_y = 0$. Therefore, (1) simplifies to

$$\Delta H_y = \varepsilon_0 j\omega \chi_{ee}^{zz} E_{z,av} + jk_0 \chi_{em}^{yy} H_{y,av}, \quad (8a)$$

$$\Delta E_z = \mu_0 j\omega \chi_{mm}^{yy} H_{y,av} + jk_0 \chi_{me}^{zz} E_{z,av}. \quad (8b)$$

Next, converting this equation into time domain by replacing $j\omega$ by $\frac{d}{dt}$ results

$$\Delta H_y = \varepsilon_0 \frac{dP_{ee}^{zz}}{dt} + \varepsilon_0 \frac{dP_{em}^{yy}}{dt}, \quad (9a)$$

$$\Delta E_z = \mu_0 \frac{dM_{mm}^{yy}}{dt} + \mu_0 \frac{dM_{me}^{zz}}{dt}, \quad (9b)$$

where auxiliary P and M functions are defined as

$$P_{ee}^{zz} = \chi_{ee}^{zz} E_{z,av}, \quad (10a)$$

$$P_{em}^{yy} = \sqrt{\frac{\mu_0}{\varepsilon_0}} \chi_{em}^{yy} H_{y,av}, \quad (10b)$$

$$M_{mm}^{yy} = \chi_{mm}^{yy} H_{y,av}, \quad (10c)$$

$$M_{me}^{zz} = \sqrt{\frac{\varepsilon_0}{\mu_0}} \chi_{me}^{zz} E_{z,av}. \quad (10d)$$

From (9a), $H_y^{n-\frac{1}{2}}(0^+)$ in equation (5) is found as

$$H_y^{n-\frac{1}{2}}(0^+) = H_y^{n-\frac{1}{2}}(k) + \frac{\varepsilon_0}{\Delta t} \left[P_{ee}^{zz,n} - P_{ee}^{zz,n-1} + P_{em}^{yy,n-\frac{1}{2}} - P_{em}^{yy,n-\frac{3}{2}} \right]. \quad (11)$$

Substitution of this equation into (5) yields

$$E_z^n(k+1) = E_z^{n-1}(k+1) + \frac{\Delta t}{\varepsilon_0 \Delta x} \left[H_y^{n-\frac{1}{2}}(k+1) - H_y^{n-\frac{1}{2}}(k) \right] - \frac{1}{\Delta x} \left(P_{ee}^{zz,n} - P_{ee}^{zz,n-1} + P_{em}^{yy,n-\frac{1}{2}} - P_{em}^{yy,n-\frac{3}{2}} \right). \quad (12)$$

P_s are found by discretization of (10a) and (10b) which yields

$$P_{ee}^{zz,n+1} = B_{ee} P_{ee}^{zz,n} + C_{ee} P_{ee}^{zz,n-1} + D_{ee} \frac{E_z^n(k) + E_z^n(k+1)}{2}, \quad (13a)$$

$$P_{em}^{yy,n+\frac{1}{2}} = B_{em} P_{em}^{yy,n-\frac{1}{2}} + C_{em} P_{em}^{yy,n-\frac{3}{2}} + D_{em} \frac{H_y^{n-\frac{1}{2}}(k) + H_y^{n-\frac{1}{2}}(k+1)}{2}, \quad (13b)$$

where $B_{kk} = \frac{2-\omega_{p,kk}^2 dt^2}{1+\delta_{p,kk} dt}$, $C_{kk} = -\frac{1-\delta_{p,kk} dt}{1+\delta_{p,kk} dt}$, $D_{ee} = \frac{\Delta\varepsilon_p \omega_{p,kk}^2 dt^2}{2+2\delta_{p,kk} dt}$ and $D_{em} = D_{ee}\eta_0$.

In a similar fashion $E_z(0^-)$ can be found by discretization of (9b) which yields

$$E_z^n(0^-) = E_z^n(k+1) - \frac{\mu_0}{\Delta t} \left[M_{mm}^{yy,n+\frac{1}{2}} - M_{mm}^{yy,n-\frac{1}{2}} \right] - \frac{\mu_0}{\Delta t} \left[M_{me}^{zz,n} - M_{me}^{zz,n-1} \right]. \quad (14)$$

Substitution of this equation into (4) results

$$H_y^{n+\frac{1}{2}}(k) = H_y^{n-\frac{1}{2}}(k) + \frac{\Delta t}{\mu_0 \Delta x} [E_z^n(k+1) - E_z^n(k)] - \frac{1}{\Delta x} \left[M_{mm}^{yy,n+\frac{1}{2}} - M_{mm}^{yy,n-\frac{1}{2}} + M_{me}^{zz,n} - M_{me}^{zz,n-1} \right], \quad (15)$$

where

$$M_{mm}^{yy,n+\frac{3}{2}} = B_{mm} M_{mm}^{yy,n+\frac{1}{2}} + C_{mm} M_{mm}^{yy,n-\frac{1}{2}} + D_{mm} H_{y,av}^{n+\frac{1}{2}} \quad (16a)$$

$$M_{me}^{zz,n+1} = B_{me} M_{me}^{zz,n} + C_{me} M_{me}^{zz,n-1} + D_{me} E_{z,av}^n, \quad (16b)$$

with $D_{me} = \frac{D_{ee}}{\eta_0}$.

V. SIMULATION RESULTS

In this section, we demonstrate two examples of dispersive metasurface to show the applicability of the proposed method. The first example is a Lorentzian dispersive metasurface and the second example is Debye dispersive metasurface.

For Lorentzian metasurface of (7), we assume isotropic electric and magnetic susceptibilities are equal – thus, no reflection – and the dispersion parameters are given by $\Delta\varepsilon_p = 1.5$, $\omega_{p,kk} = 2\pi 20$ and $\delta_{p,kk} = 0.1\omega_{p,kk}$. Note that, the normalized parameters $\varepsilon_0 = \mu_0 = c_0 = 1$ where c_0 is the velocity of light in free space, is used. The metasurface is invariant in all directions, therefore, we be analyzed using 1D FDTD code. It is illuminated by a plane wave of unit amplitude with normalized frequency of $f = 1\text{Hz}$.

The simulation result is shown in Fig. 4. As expected there is no field in the transmitted field region since the electric and magnetic susceptibilities are equal. The transmitted field is phase shifted compared to the incident field with unit amplitude.

The second example is a metasurface with Debye dispersion characteristic given by (2), $\chi_{D,ee}^{yy} = \frac{\Delta\varepsilon_{p,ee}}{1+j\omega\tau_{ee}}$ and $\chi_{D,mm}^{xx} = \frac{\Delta\varepsilon_{p,mm}}{1+j\omega\tau_{mm}}$ where $\Delta\varepsilon_{p,ee} = 2.5$, $\Delta\varepsilon_{p,mm} = 0.5$, $\tau_{ee} = 70\Delta t$ and $\tau_{mm} = 60\Delta t$ with $\Delta t = 5.9\text{ms}$. In this example, we have used same normalization as the

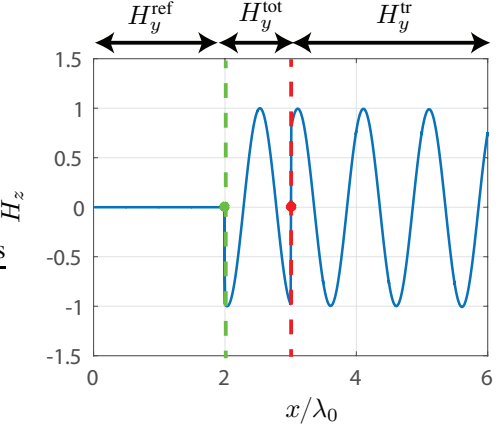


Fig. 3: Simulation result of the Lorentzian dispersive metasurface. The metasurface is shown by red mark and positioned at $x/\lambda_0 = 3$. It is illuminated by a plane wave source shown by green mark and positioned at $x/\lambda_0 = 2$.

previous example. The metasurface is illuminated by a plane wave source and since the electric and magnetic susceptibilities are not equal, the reflection should be non-zero. This result is in excellent agreement with the

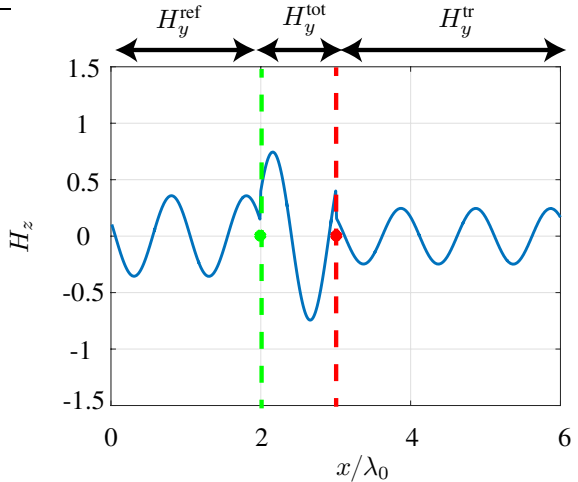


Fig. 4: Simulation result of the Debye dispersive metasurface. The metasurface is shown by red mark and positioned at $x/\lambda_0 = 3$ and illuminated by a plane wave source shown by green mark, positioned at $x/\lambda_0 = 2$.

frequency domain analytic result from which the reflected and transmitted fields amplitude is $R = 0.355$ and $T = 0.2466$, respectively. From Fig. 4, $R = 0.3575$ and $T = 0.246$ which is very close to the analytic frequency domain results. Note that, since the metasurface is lossy, therefore, $R + T \neq 1$.

VI. CONCLUSION

GSTC-FDTD was developed for analysis of general dispersive metasurface simulation. To take into account the metasurface zero-thickness effect, virtual nodes are added around the metasurface. Only the update equation for the fields around the metasurface needs to be modified. Auxiliary functions are added to make the GSTC equations discretizable. The proposed technique was proved by two examples.

REFERENCES

- [1] N. Yu, P. Genevet, M. A. Kats, F. Aieta, J.-P. Tetienne, F. Capasso, and Z. Gaburro, "Light propagation with phase discontinuities: generalized laws of reflection and refraction," *Science*, vol. 334, no. 6054, pp. 333–337, 2011.
- [2] S. Jahani and Z. Jacob, "All-dielectric metamaterials," *Nat. Nanotechnol.*, vol. 11, no. 1, p. 23, 2016.
- [3] Y. Liu and X. Zhang, "Metasurfaces for manipulating surface plasmons," *Appl. Phys. Lett.*, vol. 103, no. 14, p. 141101, 2013.
- [4] A. V. Kildishev, A. Boltasseva, and V. M. Shalaev, "Planar photonics with metasurfaces," *Science*, vol. 339, no. 6125, p. 1232009, 2013.
- [5] F. Monticone, C. A. Valagiannopoulos, and A. Alù, "Parity-time symmetric nonlocal metasurfaces: all-angle negative refraction and volumetric imaging," *Phys. Rev. X*, vol. 6, no. 4, p. 041018, 2016.
- [6] C. Caloz, M. Salem, and K. Achouri, "Metasurfaces for moulding waves: Synthesis and implementation roads," in *Advanced Electromagnetic Materials in Microwaves and Optics (METAMATERIALS), 2014 8th International Congress on*. IEEE, 2014, pp. 73–75.
- [7] C. Maurer, A. Jesacher, S. Fürhapter, S. Bernet, and M. Ritsch-Marte, "Tailoring of arbitrary optical vector beams," *New J. Phys.*, vol. 9, no. 3, p. 78, 2007.
- [8] X. Li, S. Xiao, B. Cai, Q. He, T. J. Cui, and L. Zhou, "Flat metasurfaces to focus electromagnetic waves in reflection geometry," *Opt. Lett.*, vol. 37, no. 23, pp. 4940–4942, 2012.
- [9] K. Achouri, M. Salem, and C. Caloz, "General metasurface synthesis based on susceptibility tensors," *IEEE Trans. Antennas Propag.*, vol. 63, no. 7, pp. 2977–2991, July 2015.
- [10] C. L. Holloway, D. C. Love, E. F. Kuester, J. A. Gordon, and D. A. Hill, "Use of generalized sheet transition conditions to model guided waves on metasurfaces/metafilms," *IEEE Trans. Antennas Propag.*, vol. 60, no. 11, pp. 5173–5186, 2012.
- [11] M. Selvanayagam and G. V. Eleftheriades, "Discontinuous electromagnetic fields using orthogonal electric and magnetic currents for waveform manipulation," *Opt. Express*, vol. 21, no. 12, pp. 14 409–14 429, 2013.
- [12] M. M. Idemen, *Discontinuities in the electromagnetic field*. John Wiley & Sons, 2011.
- [13] E. F. Kuester, M. Mohamed, M. Piket-May, and C. Holloway, "Averaged transition conditions for electromagnetic fields at a metafilm," *IEEE Trans. Antennas Propag.*, vol. 51, no. 10, pp. 2641–2651, Oct 2003.
- [14] Y. Vahabzadeh, K. Achouri, and C. Caloz, "Simulation of metasurfaces in finite difference techniques," *IEEE Trans. Antennas Propag.*, vol. 64, no. 11, pp. 4753–4759, Nov 2016.
- [15] S. Sandeep, J. M. Jin, and C. Caloz, "Finite-element modeling of metasurfaces with generalized sheet transition conditions," *IEEE Trans. Antennas Propag.*, vol. 65, no. 5, pp. 2413–2420, May 2017.
- [16] T. J. Smy, S. Stewart, and S. Gupta, "Integrated generalized sheet transition conditions (GSTCs) in a yee-cell based finite-difference time-domain (FDTD) simulation of electromagnetic metasurfaces," *arXiv:1706.10136*, Jun. 2017.
- [17] Y. Vahabzadeh, N. Chamanara, and C. Caloz, "Generalized sheet transition condition FDTD simulation of metasurface," *arXiv:1701.08760*, May 2017.
- [18] A. Taflove and S. C. Hagness, *Computational Electrodynamics: The Finite-Difference Time-domain Method*. Artech House, 2005.
- [19] V. Nayyeri, M. Soleimani, and O. M. Ramahi, "Modeling graphene in the finite-difference time-domain method using a surface boundary condition," *IEEE Trans. Antennas and Propag.*, vol. 61, no. 8, pp. 4176–4182, Aug 2013.